Int. J. Curr. Res. Med. Sci. (2025). 11(6): 27–39

International Journal of Current Research in Medical Sciences

ISSN: 2454-5716

(A Peer Reviewed, Indexed and Open Access Journal)

www.ijcrims.com

Original Research Article

Volume 11, Issue 6 -2025

DOI: http://dx.doi.org/10.22192/ijcrms.2025.11.06.003

Green synthesis and optimization of *Carissa carandas* Linn. Silver nanoparticles for diabetic treatment

Mr. I. Sathish[1], Mr. Raja. V[2]

[1]M.Pharm, Associate Professor, Department of Pharmaceutics, Takshashila University, Ongur, Tindivanam, Tamilnadu, India.*sathishpharm14@gmail.com*

[2]M.Pharm, Associate Professor, Department of Pharmaceutics, S. R. I College of Pharmacy, Birudhur, Vandavasi, Tamilnadu, India.*rajvraja09@gmail.com*

Corresponding Author: Mr.I.Sathish

M.Pharm, Associate Professor, Department of pharmaceutics, Takshashila University, Ongur, Tindivanam, Tamilnadu, India.*sathishpharm14@gmail.com*

Abstract

Background:

Green synthesis of silver nanoparticles (AgNPs) using medicinal plants has emerged as a promising, eco-friendly approach for therapeutic nanoparticle development. *Carissa carandas* L., traditionally known for its antidiabetic properties, was selected for the biosynthesis of AgNPs and subsequent in-vitro evaluation

Methods:

Aqueous root extract of *Carissa carandas* was used to synthesize AgNPs via microwave-assisted reduction of silver nitrate. The synthesis was optimized using Taguchi design (L9 orthogonal array). Nanoparticles were characterized using UV-Vis spectroscopy, FTIR, SEM, particle size analysis, and zeta potential measurements. Drug content and release were assessed via UV-spectroscopy, and kinetic modeling was performed. Antidiabetic activity was evaluated using an α-amylase inhibition assay, with Acarbose as the standard.

Results:

Phytochemical screening confirmed the presence of flavonoids, phenols, and glycosides contributing to AgNP formation. Optimized nanoparticles exhibited spherical morphology, average particle size of ~684.9 nm (DLS), zeta potential of –17.8 mV, and strong SPR at 435 nm. Drug entrapment ranged from 80–83%, and formulation F9 showed sustained release (86.3% at 24 hours). Kinetic modeling indicated Higuchi and first-order release profiles. AgNPs demonstrated dose-dependent α-amylase inhibition (up to 72.73% at 800 µg/mL), comparable to Acarbose (77.19%).

Conclusion:
Green-synthesized AgNPs from *Carissa carandas* root extract showed good antidiabetic potential and sustained drug release, supporting their use in natural diabetes management.

Keywords: *Carissa carandas*, silver nanoparticles, green synthesis, microwave irradiation, drug release, α-amylase inhibition, antidiabetic activity

Introduction

Nanotechnology has revolutionized the field of medicine, especially in drug delivery and diagnostics. Among various types of nanoparticles, silver nanoparticles (AgNPs) have attracted considerable attention due to their unique physicochemical properties and broad-spectrum biological activities. Traditionally, chemical and physical methods are used to synthesize AgNPs; however, these methods often involve toxic chemicals and high energy consumption. To overcome these challenges, green synthesis using plant-based extracts offers an eco-friendly, cost-effective, and sustainable alternative. Plant extracts act as natural reducing and capping agents due to their rich phytochemical content.[1,2].

Carissa carandas L., commonly known as karonda, is a well-known medicinal plant in traditional systems of medicine, particularly used for its antidiabetic, antioxidant, and antimicrobial properties. Its roots are rich in alkaloids, flavonoids, phenols, and tannins, which not only provide therapeutic effects but also assist in the biosynthesis of nanoparticles. Using such bioresources for nanoparticle synthesis can reduce toxicity and enhance biocompatibility.[3,4]

The current study explores the microwave-assisted green synthesis of silver nanoparticles using aqueous root extract of *Carissa carandas*. Microwave heating offers rapid and uniform energy transfer, improving reaction rates and controlling particle size. Optimization was performed using Taguchi design, a robust statistical tool for determining the influence of synthesis parameters such as silver nitrate concentration and microwave exposure time on nanoparticle yield.[5,6]

The synthesized nanoparticles were evaluated for their physicochemical characteristics, drug content, release behavior, and antidiabetic activity through α-amylase inhibition assay. This study aims to establish a natural, effective, and scalable approach for developing antidiabetic nanoformulations using *Carissa carandas* extract, paving the way for alternative therapies in diabetes management.[7,8]

Materials and Methods

1. Materials

- **Plant Material**: Roots of *Carissa carandas* L. were collected from Villupuram, Tamil Nadu, India.
- **Chemicals**: Silver nitrate (Qualigens Fine Chemicals), DNSA, sodium potassium tartrate, sodium hydroxide, α-amylase enzyme (Himedia), starch, and other reagents were of analytical grade.
- **Instruments Used**: UV-Visible spectrophotometer (JASCO V-4100), FTIR spectrometer (JASCO 4100), pH meter (EUTECH), Zeta Sizer (Malvern), Scanning Electron Microscope (Hitachi X650), and magnetic stirrer (REMI-2MLH).

2. Authentication and Extraction of Plant Material

Roots of *Carissa carandas* L. were authenticated by Dr. C. Murugan, Botanical Survey of India, Southern Regional Centre, Coimbatore. The roots were washed, shade dried (<40°C), and ground into coarse powder. Aqueous extract was prepared by cold maceration: 52.709 g of root powder was soaked in 500 mL distilled water for 72 hours with intermittent shaking. The filtrate was

collected using muslin cloth and stored for further use.

3. Phytochemical Screening

Preliminary qualitative phytochemical tests were performed using standard procedures to detect the presence of:

- Alkaloids (Wagner's and Hager's test)
- Amino acids (Ninhydrin test)
- Flavonoids (Alkaline reagent, Magnesium turnings test)
- Carbohydrates (Molisch's test)
- Glycosides (Keller-Killani test)
- Tannins (Lead acetate and ferric chloride test)
- Phenols and Proteins (Xanthoproteic test)
- Terpenoids (Copper acetate test)

4. Preformulation Studies

4.1 Solubility Study

Solubility of the root extract was tested in ethanol, water, chloroform, and diethyl ether.

4.2 UV Spectral Analysis

A diluted extract (0.5 mL in 10 mL phosphate buffer pH 6.8) was scanned using a UV-Visible spectrophotometer in the range of 200–400 nm.

4.3 Standard Calibration Curve

A stock solution of the extract (1 mg/mL) was serially diluted to obtain concentrations of 4–40 µg/mL. Absorbance was measured at 215 nm to create the calibration curve.

5. Green Synthesis of Silver Nanoparticles

5.1 Preparation of Reagents

- **Extract Stock**: 1 mg of aqueous extract was diluted to 10 mL with distilled water.
- **Silver Nitrate Solution**: 0.025 g of $AgNO_3$ was dissolved in 50 mL distilled water (3 mM solution).

5.2 Synthesis

5 mL of plant extract was added dropwise to 20 mL of silver nitrate solution with continuous stirring. The mixture was subjected to microwave irradiation at varying durations (30, 60, and 90 seconds). A color change from light yellow to brown indicated nanoparticle formation.

5.3 Optimization

Synthesis was optimized using Taguchi Design via Minitab 18, considering silver nitrate concentration and microwave duration as independent variables and nanoparticle yield as the dependent variable.

6. Characterization of Nanoparticles

6.1 Visual Observation

Color change was recorded as a preliminary indicator of nanoparticle formation.

6.2 UV-Visible Spectroscopy

UV absorbance was measured in the range of 200–800 nm. Surface plasmon resonance peak around 435 nm confirmed silver nanoparticle synthesis.

6.3 FTIR Analysis

FTIR spectra of the dried plant extract, silver nitrate, and synthesized nanoparticles were recorded (4000–400 cm^{-1}) to identify functional groups responsible for reduction and stabilization.

6.4 Particle Size and Zeta Potential

Measurements were performed using Malvern Zeta Sizer. Nanoparticles were dispersed in distilled water before analysis.

6.5 Scanning Electron Microscopy (SEM)

SEM imaging was performed to study the morphology and surface characteristics of the nanoparticles.

7. Drug Content Determination

Nanoparticles equivalent to 100 mg of extract were dissolved in phosphate buffer (pH 6.8). After dilution, absorbance was measured at 215 nm and drug content was calculated using the calibration curve.

8. In-vitro Drug Release Study

A dialysis bag diffusion method was used. Nanoparticles were placed in activated dialysis membranes (MW cut-off 12,000–14,000 Da) and suspended in 100 mL phosphate buffer (pH 6.8). Samples (1 mL) were withdrawn at predetermined intervals and replaced with fresh buffer. Absorbance at 215 nm was recorded. Kinetic modeling (zero-order, first-order, Higuchi, Korsmeyer-Peppas) was done using DD Solver software.

9. In-vitro Antidiabetic Activity (α-Amylase Inhibition Assay)

Nanoparticle solutions at different concentrations (50–800 µg/mL) were incubated with α-amylase enzyme (0.5 mg/mL) and 1% starch at 37°C. After incubation, DNSA reagent was added and boiled for color development. Absorbance was measured at 540 nm. Inhibition percentage was calculated using:

Inhibition (%)=(A control−A test A control)×100\text{Inhibition (\%)} = \left(\frac{A_{\text{control}} - A_{\text{test}}}{A_{\text{control}}} \right) \times 100Inhibition (%)=(A control A control−A test)×100

Positive Control: Acarbose

Results

Table 1: Phytochemical Screening of *Carissa carandas* Aqueous Root Extract

Description: This table outlines the specific phytochemical constituents present in the aqueous root extract, their testing method, observed result, and conclusion

S. No	Constituents	Test Applied	Observation	Results
1	Alkaloids	Wagner Test	Brown reddish precipitate	Positive
		Hager's Test	Slight yellow precipitate	Positive
2	Amino Acids	Ninhydrin Test	Blue color	Positive
3	Carbohydrates	Molisch's Test	Violet ring	Positive
4	Flavonoids	Alkaline Reagent Test	Yellow color	Positive
		Ammonium Hydroxide Test	Yellow color fluorescence	Positive
		Magnesium Turning Test	Red color	Positive
5	Glycosides	Keller-Killani Test	Brown colored ring	Positive
6	Tannins	Lead Acetate Test	Yellowish precipitate	Positive
		Ferric Chloride Test	Bluish black color	Positive
7	Proteins	Xanthoproteic Test	Yellow color	Positive
8	Di-terpenes	Copper Acetate Test	Emerald green color	Positive
9	Phenols	Ferric Chloride Test	Bluish black color	Positive

Table 2: Solubility of Root Powder in Various Solvents

Description: Evaluates solubility of root powder in four common solvents to inform extraction strategy.

S. No	Solvent	Solubility
1	Ethanol	Soluble
2	Water	Soluble
3	Chloroform	Insoluble
4	Diethyl Ether	Insoluble

Table 3: UV Spectral Characteristics of Aqueous Root Extract

The maximum absorption of *Carissa carandas* L. root extract was observed at 215 nm and hence selected as the wavelength for further studies.

Parameter	Result
λmax (nm)	215 nm
Absorbance peak	Detected
Solvent used	Phosphate buffer (pH 6.8)

Table 4: FTIR Interpretation

This FTIR interpretation table summarizes functional groups present in *Carissa carandas* root extract, silver nitrate, and their mixture. It confirms the presence of alcohols, phenols, amines, alkenes, and nitro compounds. These groups contribute to the reduction and stabilization of silver nanoparticles, indicating chemical compatibility and successful nanoparticle synthesis.

Material	Standard Wavenumber Range (cm^{-1})	Observed Wavenumber (cm^{-1})	Assigned Functional Group / Inference
Carissa carandas Linn root	3600–3650	3645.49	O–H stretching – monomeric alcohols and phenols
	3300–3500	3463.53	N–H stretching – amines
	1620–1680	1639.25	C=C stretching – alkenes
	1330–1540	1384.62	N–O stretching – nitro compounds
	600–1500	757.88	C–H bending – alkanes
	600–500	546.72	C–H bending – alkanes
Silver Nitrate	3700–3584	3648.66	O–H stretching – alcohols and phenols
	3550–3200	3446.17	N–H stretching – amines
	3200–2700	2925.48	O–H stretching – alcohols
	1550–1500	1541.81	N–O stretching – nitro compounds
Mixture (Root + Silver Nitrate)	3700–3584	3620.7	O–H stretching – alcohols and phenols
	3600–3200	3428.81	N–H stretching – amines
	1620–1680	1631.48	C=C stretching – alkenes
	1330–1540	1383.68	N–O stretching – nitro compounds

Green synthesis and optimization of *Carissa carandas* L. silver nanoparticles

Silver nanoparticles were synthesized by slowly adding silver nitrate solution to *Carissa carandas* root extract under continuous stirring. No color change was observed initially. Microwave heating for 30 seconds caused a slight color change, while intense brown coloration was observed at 60–90 seconds, indicating formation of silver nanoparticles.

Table:5 Formulation of *Carissa carandas* silver nanoparticles

This table outlines the composition of 9 nanoparticle formulations using different concentrations of silver nitrate and varying microwave irradiation times.

Content	F1	F2	F3	F4	F5	F6	F7	F8	F9
***Carissa carandas* Root extract(ml)**	50	50	50	50	50	50	50	50	50
Silver nitrate (1mM)(ml)	200	–	–	200	–	–	200	–	–
Silver Nitrate (2mM)(ml)	–	200	–	–	200	–	–	200	–
Silver Nitrate (3mM)(ml)	–	-	200	–	–	200	–		200
Microwaves heating time(Seconds)	30	30	30	60	60	60	90	90	90
Yield(mg)	447	453	465	441	460	472	448	482	521

Taguchi design-based optimization

The synthesis process was optimized using **Taguchi L9 orthogonal array**, considering two independent variables:

- **A (Silver nitrate concentration)** – 3 levels: 1 mM, 2 mM, 3 mM
- **B (Microwave time)** – 3 levels: 30 sec, 60 sec, 90 sec

The **dependent variable** was the **yield** of synthesized silver nanoparticles.

Table 6: Taguchi Orthogonal Array and Yield Output

Run	Silver Nitrate (mM)	Microwave Time (sec)	Yield (mg)
1	1	30	465
2	1	60	441
3	1	90	465
4	2	30	441
5	2	60	460
6	2	90	472
7	3	30	448
8	3	60	482
9	3	90	521

Description: This table represents the Taguchi experimental matrix and nanoparticle yield for each run. The data clearly shows that both increasing silver nitrate concentration and microwave time positively impact nanoparticle yield. The highest yield (521 mg) was achieved at 3 mM concentration and 90 seconds microwave exposure (Run 9).

Table 7: Response Table for Means (Taguchi Optimization Output)

Level	Factor A (Silver Nitrate mM)	Factor B (Microwave Time sec)
1	445.3	455.0
2	465.0	457.7
3	486.0	483.7
Delta	40.7	28.7
Rank	1	2

Description: This table presents the average yields at each level of factors A and B, the delta (difference between highest and lowest values), and the rank of influence. Factor A (silver nitrate concentration) had a stronger effect on yield than microwave time, as indicated by a higher delta value of 40.7.

Characterization of synthesized silver nanoparticles (AGNPS)

The synthesized silver nanoparticles were characterized using visual observation, UV–Visible spectroscopy, FTIR analysis, SEM, particle size analysis, and zeta potential analysis to confirm their successful formation, chemical interaction, size, shape, and stability.

Visual Observation

The reaction mixture showed a **color change from pale yellow to light brown** after 30 seconds of microwave irradiation. With continued heating for 60 to 90 seconds, the solution turned **intense brown**, indicating the reduction of silver ions (Ag^{+}) to silver nanoparticles (Ag^{0}). This characteristic change is attributed to the excitation of surface plasmon vibrations in silver nanoparticles.

UV–Visible Spectroscopy

A sharp absorption peak was observed at **435 nm** using UV–Visible spectrophotometry. This peak corresponds to the surface plasmon resonance (SPR) band of silver nanoparticles.

Table 8: UV–Visible Spectroscopy Data

Parameter	Observation
Peak Wavelength (λmax)	435 nm
Spectral Range Scanned	200–800 nm
Inference	SPR confirms presence of AgNPs

Fourier-Transform Infrared (FTIR) Spectroscopy

FTIR spectroscopy was used to identify the functional groups responsible for the reduction and stabilization of silver ions. Results for the extract alone, silver nitrate alone, and their mixture are summarized below.

Table 9: FTIR Interpretation of Synthesized Silver Nanoparticles

Material	Standard Range (cm^{-1})	Observed Peak (cm^{-1})	Functional Group / Inference
Carissa carandas root extract	3600–3650	3645.49	O–H stretching (alcohols, phenols)
	3300–3500	3463.53	N–H stretching (amines)
	1620–1680	1639.25	C=C stretching (alkenes)
	1330–1540	1384.62	N–O stretching (nitro compound)
	600–1500	757.88	C–H bending (alkanes)
	500–600	546.72	C–H bending (alkanes)
Silver Nitrate	3700–3584	3648.66	O–H stretching (alcohols and phenols)
	3550–3200	3446.17	N–H stretching (amines)
	3200–2700	2925.48	O–H alcohol stretching
	1550–1500	1541.81	N–O stretching (nitro compound)
Mixture (Extract + $AgNO_3$)	3700–3584	3620.7	O–H stretching (alcohols and phenols)
	3600–3200	3428.81	N–H stretching (amines)
	1620–1680	1631.48	C=C stretching (alkenes)
	1330–1540	1383.68	N–O stretching (nitro compound)

Description: FTIR analysis revealed the presence of hydroxyl, amine, carbonyl, and nitro functional groups. Their appearance in both extract and nanoparticle spectra suggests they played a role in both **reducing silver ions** and **capping the nanoparticles**, stabilizing the system.

Particle Size Analysis

Table 10: Particle Size Analysis

Parameter	Value
Average Particle Size	684.9 nm
Polydispersity Index (PDI)	0.307
Intercept	0.878

This table summarizes particle size results indicating moderate polydispersity and potential aggregation or plant compound capping.

Zeta Potential Analysis

Table 11: Zeta Potential Analysis

Parameter	Value
Zeta Potential (mV)	–17.8 mV
Peak Area	100% intensity

This table shows the moderate stability of the AgNP colloidal suspension due to phytochemical surface interaction.

Scanning Electron Microscopy (SEM)

- Magnification Used: 55,000×
- Shape: Spherical, well-defined
- Size Range (Observed by SEM):
  - 42.56 nm
  - 47.27 nm
  - 41.46 nm
  - 43.79 nm
  - 54.55 nm
  - 59.97 nm

Despite the higher average size from DLS, SEM confirms nanosized particles in the range of ~40–60 nm with spherical shape and smooth surfaces, suggesting effective nucleation and good morphology.

Figure: 1 SEM analysis of *Carissa carandas* L. silver nanoparticles

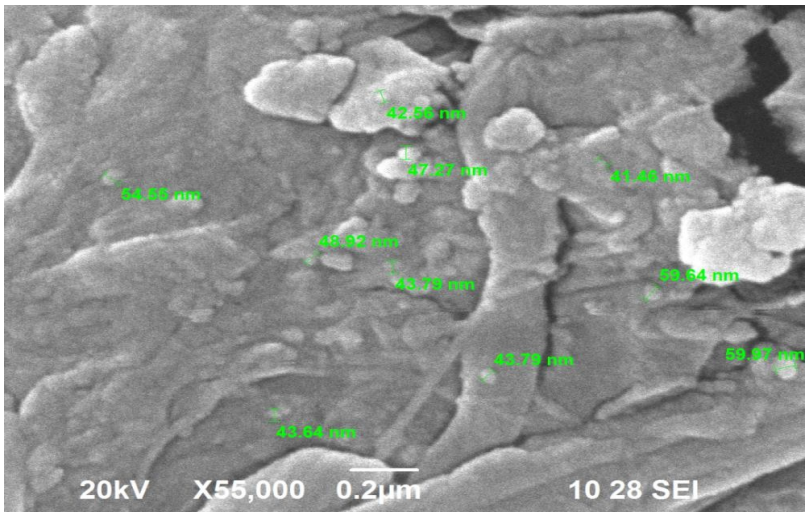

Drug content

Table 12: Drug Content of Selected AgNP Formulations

Formulation	Drug Content (%)
F6	82.67
F7	80.72
F8	83.46
F9	83.36

All selected formulations showed high drug entrapment efficiency, suitable for in vitro release studies.

In-vitro drug release study

Table 13: In Vitro Drug Release of ***Carissa carandas*** L. Silver Nanoparticles (%)

Time (hr)	F3	F6	F8	F9
0	0.00	0.00	0.00	0.00
1	7.51	10.5	10.4	7.7
2	11.21	19.2	12.06	13.1
4	26.68	34.4	25.1	22.3
6	37.5	42.1	38.1	35.4
8	45.33	52.0	52.8	51.2
12	56.4	61.4	68.7	73.2
24	63.4	68.2	76.1	86.3

This *table shows the cumulative drug release. F9 demonstrated the most sustained and extended release profile across 24 hours.*

Drug release kinetics model fitting results

Evaluates fit of release data to different kinetic models for understanding the mechanism of drug release.

Table 14:R^2 Value Obtained For Various Kinetic Release Models:

Formulation	Zeroorder kinetics R^2	First order kinetic R^2	Higuchi's kinetic R^2	Korsmayer peppas kinetic	
				R^2	n
F3	0.7075	0.8983	0.9529	0.9535	0.518
F6	0.5161	0.8250	0.9401	0.9519	0.429
F8	0.7624	0.9560	0.9417	0.9470	0.560
F9	0.8062	0.9786	0.9364	0.9502	0.596

The release of *Carissa carandas* L. silver nanoparticles were best fitted into Higuchi's equation for the first two formulations (F3 and F6). The Higuchi's equation describes the diffusion of drug from homogenous and granular matrix systems. The release of *Carissa carandas* L. silver nanoparticles were best fitted into first order kinetics for the formulations F8 and F9. Furthermore Korsmayer peppas model describes n value of formulation F6 is 0.43(n<0.5) indicated that F6 exhibited fickian diffusion and n value of other three formulations (F3,F8 and F9) are having a value of0.5<n< 1 which indicatedformulations (F3,F8 and F9) exhibited non fickian diffusion

In-vitro antidiabetic study of synthesise *Carissa carandas* L. silver nanoparticles

Table 15: Acarbose vs. ***Carissa carandas*** L. AgNPs

Concentration (µg/mL)	% Inhibition (Acarbose)	% Inhibition (AgNPs)
50	16.34%	16.51%
100	21.53%	20.53%
200	37.87%	30.89%
400	50.67%	48.19%
800	77.19%	72.73%

Acarbose, a known α-amylase inhibitor, showed concentration-dependent enzyme inhibition, with maximum inhibition of **77.19% at 800 µg/mL**. Inhibition increased steadily, reflecting effective suppression of carbohydrate digestion. The synthesized AgNPs from *Carissa carandas* root extract exhibited significant α-amylase inhibition in a dose-dependent manner. The highest inhibition observed was **72.73% at 800 µg/mL**, indicating substantial potential as a natural antidiabetic agent. Both agents showed comparable enzyme inhibition profiles. While Acarbose had slightly higher inhibitory activity across all concentrations, the AgNPs from *Carissa carandas* demonstrated **promising natural enzyme inhibition**, suggesting potential use in postprandial glucose control with possibly fewer side effects.

Discussion

The present study aimed to develop a green synthesis protocol for silver nanoparticles (AgNPs) using the aqueous root extract of *Carissa carandas* L. and to characterize the synthesized nanoparticles for their antidiabetic potential. The experimental findings provide a multidimensional understanding of the extract's phytoconstituents, the success of the nanoparticle synthesis approach, and the biological relevance of the resulting nanoformulations.

Phytochemical Composition and Extract Properties

Phytochemical screening confirmed the presence of bioactive compounds such as alkaloids, flavonoids, glycosides, tannins, phenols, and terpenoids in the root extract. These compounds are known for their reducing and stabilizing properties, playing an essential role in the formation and surface modification of nanoparticles. The solubility profile demonstrated that the extract is soluble in both water and ethanol, reinforcing its suitability for aqueous-based green synthesis protocols. The UV spectrum showed a peak at 215 nm, which became the reference wavelength for drug content and release studies.

Synthesis and Optimization of Silver Nanoparticles

Silver nanoparticles were synthesized by treating the aqueous root extract with various concentrations of silver nitrate under microwave irradiation. The color change from pale yellow to dark brown confirmed the reduction of Ag^{+} to Ag^{0}, primarily attributed to the excitation of surface plasmon resonance (SPR), supported by UV-Visible spectroscopy with an absorption peak at 435 nm.

The synthesis process was optimized using a Taguchi L9 orthogonal array. The maximum yield (521 mg) was achieved at a silver nitrate concentration of 3 mM and microwave time of 90 seconds, indicating that both concentration and exposure duration directly impact nanoparticle yield. Among the tested variables, silver nitrate concentration exerted a more profound influence on yield than microwave time, as evident from the delta values in the response table.

Characterization of Synthesized AgNPs

FTIR analysis confirmed that functional groups such as hydroxyl, amines, alkenes, and nitro groups from the root extract were involved in both reducing silver ions and stabilizing the nanoparticles. This confirms the dual role of the extract as a reducing and capping agent. SEM analysis revealed spherical nanoparticles with smooth surfaces and a size range of 42–60 nm. However, dynamic light scattering (DLS) showed a larger average size (~684.9 nm) and moderate PDI (0.307), which can be attributed to hydrodynamic diameter and plant compound adsorption. The zeta potential of –17.8 mV indicated moderate colloidal stability due to phytochemical surface capping.

Drug Content and Release Studies

The drug content across formulations (F6–F9) ranged from 80.72% to 83.46%, demonstrating efficient drug entrapment. In-vitro drug release studies showed sustained release, with formulation F9 achieving the highest cumulative release (86.3%) at 24 hours. The prolonged release may be attributed to the effective capping of nanoparticles by phytoconstituents, which can act as rate-controlling membranes.

Kinetic modeling revealed that formulations F3 and F6 followed Higuchi kinetics ($R^2 > 0.94$), indicative of diffusion-based drug release from a matrix system. Conversely, formulations F8 and F9 showed best fit to first-order kinetics (R^2 ~0.97), implying that the drug release was concentration-dependent. The Korsmeyer-Peppas model further confirmed that formulation F6 followed Fickian diffusion ($n < 0.5$), whereas the other three (F3, F8, F9) exhibited non-Fickian (anomalous) transport ($0.5 < n < 1$), suggesting a combination of diffusion and erosion mechanisms.

In-vitro Antidiabetic Activity

The α-amylase inhibition assay demonstrated that *Carissa carandas* AgNPs inhibited enzyme activity in a dose-dependent manner, achieving up to 72.73% inhibition at 800 µg/mL. Though slightly lower than the standard drug Acarbose (77.19%), the synthesized nanoparticles exhibited promising inhibitory activity, indicating their potential as a natural and possibly safer alternative for managing postprandial hyperglycemia.

Conclusion

The present study successfully demonstrated the green synthesis of silver nanoparticles using the aqueous root extract of *Carissa carandas* L., a plant known for its traditional medicinal applications. The phytochemical constituents in the extract served as natural reducing and stabilizing agents, enabling eco-friendly nanoparticle formation under microwave irradiation. Optimization via the Taguchi design revealed that both silver nitrate concentration and microwave exposure time significantly influence nanoparticle yield.

Characterization studies confirmed the formation of spherical, moderately stable nanoparticles with appropriate particle size and surface properties. The nanoparticles exhibited high drug entrapment efficiency and a sustained release profile over 24 hours, with kinetic modeling indicating both diffusion and anomalous release mechanisms depending on formulation parameters.

Importantly, the synthesized AgNPs showed substantial α-amylase inhibition, supporting their potential as a natural antidiabetic agent. Though slightly less potent than Acarbose, the biological activity of *Carissa carandas* AgNPs highlights their therapeutic promise in managing postprandial glucose levels with possibly reduced side effects.

Overall, this study presents a novel, scalable, and environmentally friendly approach to developing biofunctional silver nanoparticles with potential applications in diabetes management and drug delivery.

References

1. Sachan and Gupta, A Review On Nanotized Herbal Drugs, International Journal of Pharmaceutical Sciences and Research, 2015; 6(3): 961-970:
2. Sadiq and Rassol. Formulation and evaluation of silibinin loaded solid lipid nanoparticles for peroral use targeting lower part of gastrointestinal tract, international journal of pharmacy and pharmaceutical science, 2014; 6: 54-67.
3. Sastry, M. Mayya, K.S. and Bandyopadhyay, K. pH Dependent changes in the optical properties of carboxylic acid derivatized silver colloidal particles. Colloids Surf. A: Physicochem. & Engi. Aspects. 1997; 127: 221–228.
4. Shah, Fawcett, Sharma and Tripathy. Green Synthesis of Metallic Nanoparticles via Biological Entities, Materials, 2015; 8(11): 7278-7308.
5. Shakeel Ahmed, Saifullah, Mudasir Ahmad, Lal Swami, et al. Green synthesis of silver nanoparticles using *Azadirachta indica* aqueous leaf extract', Journal of Radiation Research and Applied Sciences, 2016; 9: 1-7.
6. Sharma P.C, Yelne M.B and Dennis T.J. 'Database on Medicinal Plants Used in Ayurveda, 2001; 7: 369-377:
7. Singh, Rawat and Isha. Microwave-Assisted Synthesis Of Silver Nanoparticles From *OriganumMajorana* And *Citrus Sinensis*Leaf And Their Antibacterial Activity: A Green Chemistry Approach, Springer Open(Bioresour And Bioprocess). 2016; 3: 1-7.

8. Singh.P and Vidyasagar .G.M Biosynthesis, Characterization, and Antidermatophytic Activity of Silver Nanoparticles Using Raamphal Plant (*Annona reticulata*) Aqueous Leaves Extract. Indian Journal of Materials Science Volume. 2014; 1-5

Access this Article in Online	
	Website: www.ijcrims.com
Quick Response Code	Subject: Nanotechnology
DOI: 10.22192/ijcrms.2025.11.06.003	

How to cite this article:
I. Sathish, Raja. V. (2025). Green synthesis and optimization of *Carissa carandas* Linn. Silver nanoparticles for diabetic treatment. Int. J. Curr. Res. Med. Sci. 11(6): 27-39.
DOI: http://dx.doi.org/10.22192/ijcrms.2025.11.06.003